J|A|C|S
ARTICLES
Published on Web 05/16/2006

Nanotubes from a Vitamin C-Based Bolaamphiphile

Moira Ambrosi,[†] Emiliano Fratini,[†] Viveka Alfredsson,[‡] Barry W. Ninham,[†,§] Rodorico Giorgi,[†] Pierandrea Lo Nostro,*[,†] and Piero Baglioni[†]

Contribution from the Department of Chemistry and CSGI, University of Florence, 50019 Sesto Fiorentino (Firenze), Italy, Physical Chemistry 1, Center for Chemistry and Chemical Engineering, Lund University, 22100 Lund, Sweden, and Department of Applied Mathematics, Research School of Physical Sciences and Engineering, Institute of Advances Studies, Australian National University, Canberra, Australia 0200

Received November 14, 2005; E-mail: pln@csgi.unifi.it

Abstract: A bolaform surfactant, 1,12-diascorbyl dodecanedioate (BOLA12), with ascorbic acid units as the polar headgroups was synthesized for the first time. Once dispersed in water above 0.5% w/w, BOLA12 forms hollow nanotubes as revealed by cryo-TEM experiments. These nanostructures transform into clear micellar solutions on heating. X-ray diffraction and SAXS experiments were performed both on the pure solid and on its aqueous dispersions. The critical aggregation concentration and the phase behavior were determined by conductivity and DSC experiments. The latter technique provided also the amount of strongly bound, solvating water molecules that surround the polar headgroups. BOLA12 shows the same reducing properties of ascorbic acid, as indicated by the antioxidant activity evaluated with the DPPH method. This feature was used for the reduction of Pd(II) ions on the surface of the nanoassemblies, which lead to the formation of large bundles homogeneously coated with palladium as observed in SEM micrographs.

Introduction

The formation and properties of nanotubes are currently the focus of intense studies because of their potential use in chemistry, biology, and materials science.[1−3] In particular, organic nanostructures that possess electrochemical/photochemical properties, and stimuli responsiveness to external environmental changes are a main goal.[4,5] Applications for such structures are increasing. They include and span fields from membrane mimetic systems to biosensors, from drug and/or gene delivery systems to metallic nanorods for electronics.[6−14] Bolaamphiphiles, i.e. surfactant molecules that contain two hydrophilic headgroups connected by a hydrophobic spacer, appear to be excellent candidates for the production of organic supramolecular structures such as nanotubes,[1] nanofibers,[6,11] and helical ribbons.[7,9,15] In the search for the production of redox active nanostructures, we have focused our attention on one of the most powerful natural antioxidants, i.e., Vitamin C. This inhibits free radical-initiated lipid peroxidation, a process presumably implicated in a variety of chronic health problems such as aging, cancer, and cardiovascular diseases.[16,17] Ascorbic acid is poorly soluble in hydrophobic media. Thus, amphiphilic ascorbyl derivatives must be synthesized to extend their reducing properties to encompass hydrophobic environments. In previous papers, we reported the synthesis and properties of alkanoyl-6-*O*-ascorbic acid esters, (ASC*n* with n the hydrophobic chain length, $8 \leq n \leq 18$).[18−26] In these surfactants only the vitamin

[†] University of Florence.
[‡] Lund University.
[§] Australian National University.

(1) Matsui, H.; Douberly, G. E. J. *Langmuir* **2001**, *17*, 7918−7922.
(2) Ai, S.; Lu, G.; He, Q.; Li, J. *J. Am. Chem. Soc.* **2003**, *125*, 11140−11141.
(3) Chupin, V.; Killian, J. A.; de Kruijff, B. *Biophys. J.* **2003**, *84*, 2373−2381.
(4) Hong, B. H.; Lee, J. Y.; Lee, C.-H.; Kim, J. C.; Bae, S. C.; Kim, K. S. *J. Am. Chem. Soc.* **2001**, *123*, 10748−10749.
(5) Hou, S.; Wang, J.; Martin, C. R. *J. Am. Chem. Soc.* **2005**, *127*, 8586−8587.
(6) Shimizu, T.; Iwaura, R.; Masuda, M.; Hanada, T.; Yase, K. *J. Am. Chem. Soc.* **2001**, *123*, 5947−5955.
(7) Song, J.; Cheng, Q.; Kopta, S.; Stevens, R. C. *J. Am. Chem. Soc.* **2001**, *123*, 3205−3213.
(8) Djalali, R.; Chen, Y.-f.; Matsui, H. *J. Am. Chem. Soc.* **2002**, *124*, 13660−13661.
(9) Song, J.; Cheng, Q.; Stevens, R. C. *Chem. Phys. Lipids* **2002**, *114*, 203-214.
(10) Zhang, S. *Biotechnol. Adv.* **2002**, *20*, 321−339.
(11) Claussen, R. C.; Rabatic, B. M.; Stupp, S. I. *J. Am. Chem. Soc.* **2003**, *125*, 12680−12681.
(12) Pakhomov, S.; Hammer, R. P.; Mishra, B. K.; Thomas, B. N. *Proc. Natl. Acad. Sci. U.S.A.* **2003**, *100*, 3040−3042.
(13) Bianco, A.; Kostarelos, K.; Prato, M. *Curr. Opin. Chem. Biol.* **2005**, *9*, 1−6.
(14) Yang, M.; Yang, Y.; Yang, H.; Shen, G.; Yu, R. *Biomaterials* **2005**, *27*, 246−255.
(15) Shimizu, T.; Masuda, M. *J. Am. Chem. Soc.* **1997**, *119*, 2812−2818.
(16) Nihro, Y.; Miyataka, H.; Sudo, T.; Matsumoto, H.; Sathoh, T. *J. Med. Chem.* **1991**, *34*, 2152−2157.
(17) Bisby, R. H.; Parker, A. W. *J. Am. Chem. Soc.* **1995**, *117*, 5664−5670.
(18) Capuzzi, G.; Lo Nostro, P.; Kulkarni, K.; Fernandez, J. E.; Vincieri, F. F. *Langmuir* **1996**, *12*, 5413−5418.
(19) Capuzzi, G.; Lo Nostro, P.; Kulkarni, K.; Fernandez, J. E. *Langmuir* **1996**, *12*, 3957−3963.
(20) Capuzzi, G.; Kulkarni, K.; Fernandez, J. E.; Vincieri, F. F.; Lo Nostro, P. *J. Colloid Interface Sci.* **1997**, *186*, 271−279.
(21) Lo Nostro, P.; Capuzzi, G.; Pinelli, P.; Mulinacci, N.; Romani, A.; Vincieri, F. F. *Colloids Surf. A* **2000**, *167*, 83−93.
(22) Lo Nostro, P.; Capuzzi, G.; Romani, A.; Mulinacci, N. *Langmuir* **2000**, *16*, 1744−1750.
(23) Palma, S.; Manzo, R. H.; Allemandi, D.; Fratoni, L.; Lo Nostro, P. *Langmuir* **2002**, *18*, 9219−9224.
(24) Lo Nostro, P.; Ninham, B. W.; Fratoni, L.; Palma, S.; Manzo, R. H.; Allemandi, D.; Baglioni, P. *Langmuir* **2003**, *19*, 3222−3228.
(25) Lo Nostro, P.; Ninham, B. W.; Ambrosi, M.; Fratoni, L.; Palma, S.; Allemandi, D.; Baglioni, P. *Langmuir* **2003**, *19*, 9583−9591.
(26) Ambrosi, M.; Lo Nostro, P.; Fratoni, L.; Dei, L.; Ninham, B. W.; Palma, S.; Manzo, R. H.; Allemandi, D.; Baglioni, P. *Phys. Chem. Chem. Phys.* **2004**, *6*, 1401−1407.

10.1021/ja057730x CCC: $33.50

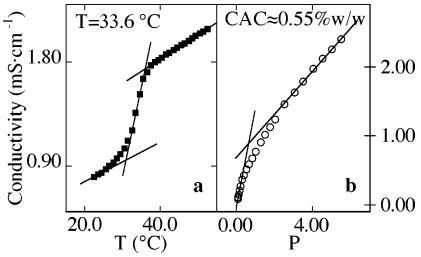

Figure 1. (a) Conductivity as a function of temperature for 4% w/w sample. The Krafft point determined was 33.6 °C. (b) Conductivity as a function of BOLA12 concentration (P% w/w). The critical aggregation concentration was about 0.55% ≈ 10 mM.

C primary −OH group is involved in the ester bond, and the other hydrophilic residues are still available for establishing hydrogen bonds and for performing redox and complexing functions.[21,22] Hydrated ASC*n* surfactants form lamellar phases (*coagels*), micelles or gel-like dispersions depending on composition, solvent nature, and temperature.[23−25] Due to their peculiar phase behavior and to their redox functionalities, these nanoassemblies represent an excellent tool for the delivery of hydrophobic and sensitive drugs.[27,28]

Here we report the synthesis of a new decamethylene-group-spanned bolaamphiphile, BOLA12, with two vitamin C rings as headgroups (Figure S1, Supporting Information). Nanotubes are found in aqueous dispersions of BOLA12 at room temperature above 0.5% w/w. X-ray diffraction (XRD), small-angle X-ray-scattering (SAXS), cryo-transmission electron microscopy (cryo-TEM), conductivity, and differential scanning calorimetry (DSC) measurements were used to explore the aggregate nanostructures. Reduction of Pd(II) on the outer surface of the BOLA12 nanotubes resulted in a homogeneous coating with palladium as shown by SEM experiments.

Results and Discussion

On dispersion in water at room temperature and above 0.5% w/w, BOLA12 produces opaque, mostly semitransparent condensed phases. Upon heating, these systems turn into a transparent homogeneous liquid.

Conductivity. The phase transition temperature (T_{trans}) and the critical aggregation concentration (CAC) were determined by conductivity (Figure 1,a and b, respectively).

A 4% w/w sample was used for the evaluation of T_{trans}. The 4% concentration was chosen to guarantee the presence of aggregates in the liquid phase after the transition, and to obtain a significant conductivity gradient. T_{trans} was assigned to the midpoint between the two intersection points as shown in Figure 1a, and comes out to be about 33.6 °C. The critical aggregation concentration (CAC) was established at 48 °C, in the concentration range between 0.05 and 5.5% w/w. The CAC was determined as the intersection point between the two straight lines that give a linear fit to the experimental conductivity data in the low and high concentration domains as shown in Figure 1b and results in about 0.55% w/w (∼10 mM).

Cryo-TEM. Figures 2 and 3 show the structures obtained from the 5% w/w sample in the condensed phase. Tubular structures are clearly seen in the micrographs. In Figure 2, the

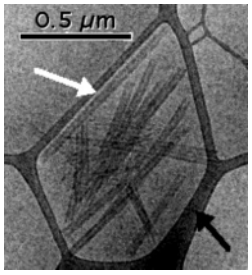

Figure 2. 5% w/w BOLA12/water sample (in the condensed phase). The white arrow points at a group of tubules. The black arrow indicates the carbon support film.

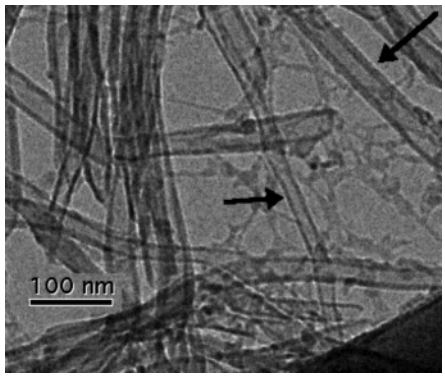

Figure 3. 5% w/w BOLA12/water sample above the phase transition temperature, plunged into the cryogene after 1−2 min to let the solvent evaporate.

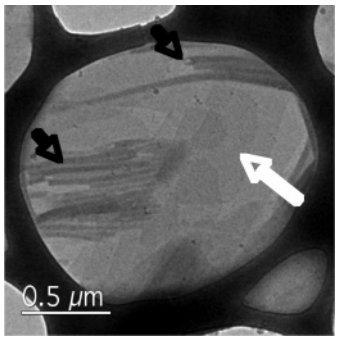

Figure 4. 10% w/w BOLA12/water placed in the CEVS at 34 °C.

sample was placed on the grid above the phase transition. After blotting the excess solution with filter paper, the sample was allowed to form the condensed phase and then plunged into the cryogene. In Figure 3, the sample was kept on the grid for 1−2 min above the phase transition temperature, before being plunged into the cryogene.

The average outer width of the tubes is about 28 nm, the mean inner diameter is about 15 nm, and the length ranges roughly between 0.2 and 1 μm. Figure 3 shows a more detailed image, as the solvent was evaporated to avoid the background from the vitreous ice. It is evident that the tubes are hollow, as shown by the nearly electron-transparent central core.[5]

A micrograph recorded from the condensed phase formed by the 10% w/w sample is reported in Figure 4. In this case, the sample was left at 34 °C on the grid for approximately 10 s to form the condensed phase. Two coexisting phases, sheetlike (white arrow) and elongated structures (black arrows), are shown.

When the 10% and 40% w/w samples were prepared at higher temperature in the CEVS (48 °C), no aggregated structures were

(27) Palma, S.; Manzo, R. H.; Allemandi, D.; Fratoni, L.; Lo Nostro, P. *J. Pharm. Sci.* **2002**, *91*, 1810−1816.
(28) Bilia, A. R.; Bergonzi, M. C.; Vincieri, F. F.; Lo Nostro, P.; Morris, G. A. *J. Pharm. Sci.* **2002**, *91*, 2265−2270.

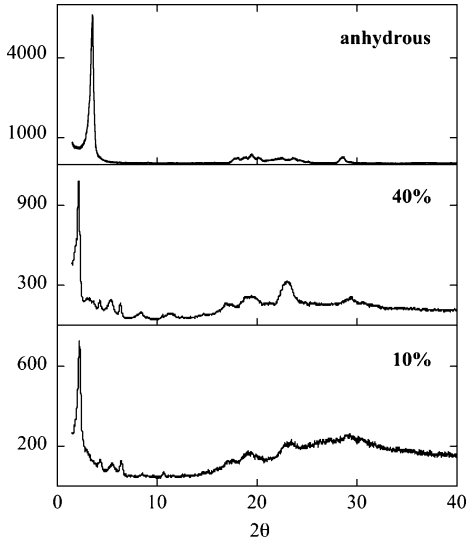

Figure 5. X-ray profiles for pure anhydrous BOLA12 and its aqueous dispersions at room temperature.

found. Below the phase transition temperature, the 40% w/w sample was too thick to be imaged.

XRD. X-ray diffraction measurements were carried out either on the pure anhydrous BOLA12 or on BOLA12/water samples between 10% and 40% w/w. The diffractograms are shown in Figure 5. The low-angle region gives information on the long-range ordering of the system. For the anhydrous sample the main peak corresponds to a spacing (*d*) of 25 Å, while for all the hydrated samples the spacing increases up to about 40 Å. Corey−Pauling−Koltun (CPK) model calculations[29] gave a value of 26 Å for the length of BOLA12 with the aliphatic chain in its fully stretched conformation. Therefore, in the dry state, BOLA12 molecules produced compact monolayers with the hydrophobic tails fully extended and perpendicular to the planes formed by the headgroups.

In the presence of water, and on the assumption that the single surfactant molecules lay perpendicularly to the interface, they form monolayers separated by a thin aqueous compartment of about 15 Å. It is interesting to note that the water interlayer has the same thickness as that found for the single headed ASC*n* derivatives,[26] and for phospholipid derivatives.[30]

SAXS. Small-angle X-ray-scattering experiments were carried out on the condensed phase as well as on the liquid sample. Figure 6 shows the SAXS profiles for pure anhydrous BOLA12 (black curve) and its aqueous dispersions at 5%, 10%, 20%, and 40% w/w at 20 °C.

The peak at $Q = 0.243$ Å^{-1} (A) for the powder corresponds to 25.5 Å. This is the length of a monomer in its fully stretched conformation, in agreement with the main signal found with the XRD experiments, and with the calculated CPK model. In the case of the hydrated condensed phases, the peak broadens and shifts to a lower *Q*, 0.195 Å^{-1} (B), and this corresponds to a lamellar structure with a repetition spacing of about 33−34 Å. This feature agrees with the presence of lamellae of hydrated solid, with a thin layer (about 8−9 Å) of hydrating water molecules that surround the headgroups of the bolaamphiphiles. Similar values were found from XRD experiments. The second

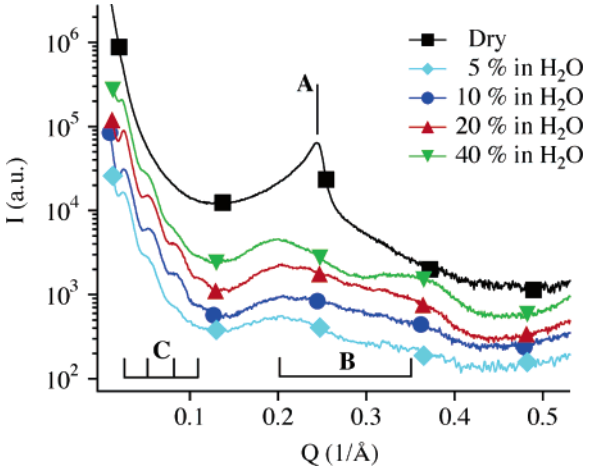

Figure 6. SAXS intensity distribution for anhydrous BOLA12 and its aqueous dispersions at room temperature. The three different ordered structures have been referred to as A (anhydrous surfactant molecule), B (hydrated surfactant molecule), and C (supramolecular assembly).

order appears at about 0.35 Å^{-1}. The peak broadening is due to the polydispersity of the aggregated structure. The extra four peaks in the range 0.022−0.115 Å^{-1} indicate the presence of very large ordered structures that are formed upon hydration. The first-order peak at about 0.022−0.025 Å^{-1} (C) corresponds to a repetition dimension ranging between 230 and 250 Å. These supramolecular structures are poorly affected by the BOLA12 concentration. Considering that a single layer of hydrated BOLA12 monomers has a thickness of 33 Å and on the basis of the inner diameter obtained from the cryo-TEM experiment, the structures that produce the "C" peak comprise hollow cylinders with a wall consisting of about 2−3 layers of hydrated surfactant molecules (Figure 7).

The nanotubes formed by BOLA12 in water dispersions produce SAXS profiles very similar to those given by lanreotide below 20%.[31] This octapeptide produces very long, hollow columns with multilayered walls, and the presence of strongly bound and interfacial water is confirmed by DSC experiments.[31]

By heating above 40 °C, the ordered condensed structures disappear, and small micellar aggregates are formed. SAXS profiles change dramatically, as illustrated in Figure 8 for the 10% w/w sample. After cooling to 20 °C the original structures are reformed. Similar results were obtained also for the 5%, 20%, and 40% w/w samples.

Figure 9 shows the SAXS profile for the 5% w/w liquid sample equilibrated at 50 °C.

The Guinier plot, i.e. ln[$I(Q)$] vs Q^2, provides a first approximation to the radius of gyration of the scattering objects:[32]

$$\ln[I(Q)] = \ln[I(0)] - \left(\frac{R_g^2}{3}\right)Q^2 \qquad (1)$$

This approximation holds for $R_gQ < 1$, in our case for $Q^2 < 0.00259$ Å^{-2}, about 40 points are in the fitting range (see inset of Figure 9). The extracted radius of gyration $R_g = 19.9 \pm 1.5$ Å is associated with a spherical micelle having an effective

(29) Koltun, W. L. *Biopolymers* **1965**, *3*, 665−679.
(30) Caffrey, M.; Hogan, J.; Rudolph, A. S. *Biochemistry* **1991**, *30*, 2134−2146.
(31) Valéry, C.; Artzner, F.; Robert, B.; Gulick, T.; Keller, G.; Grabielle-Madelmont, C.; Torres, M.-L.; Cherif-Cheikh, R.; Paternostre, M. *Biophys. J.* **2004**, *86*, 2484−2501.
(32) Guinier, A.; Fournet, G. *Small Angle Scattering of X-rays*; John Wiley: New York, 1955.

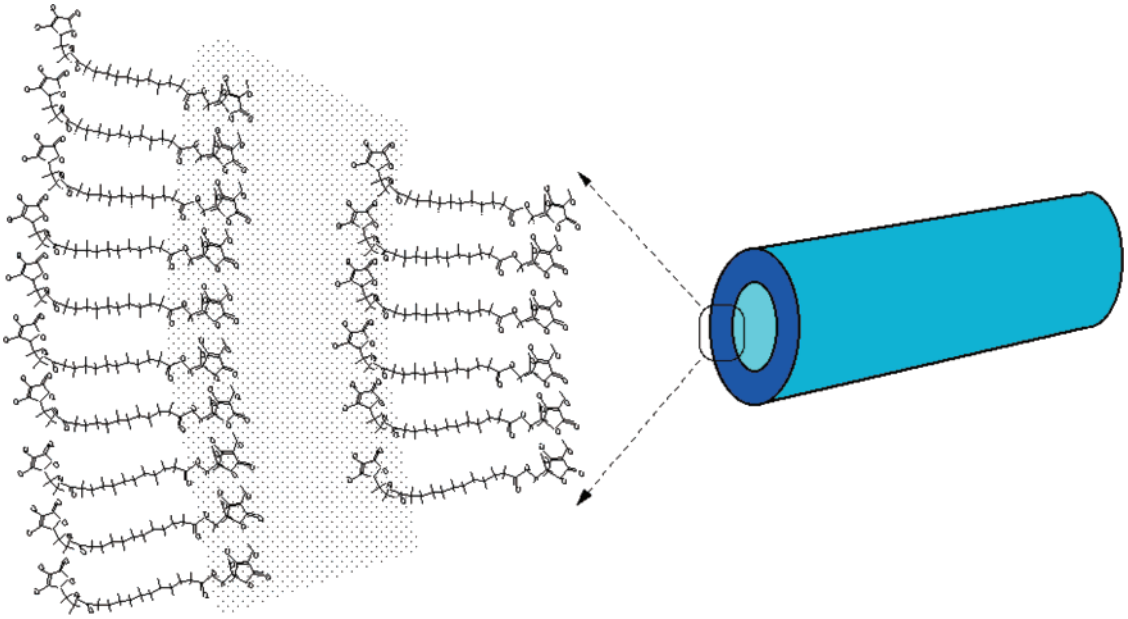

Figure 7. Schematic structure of a nanotube produced by BOLA12.

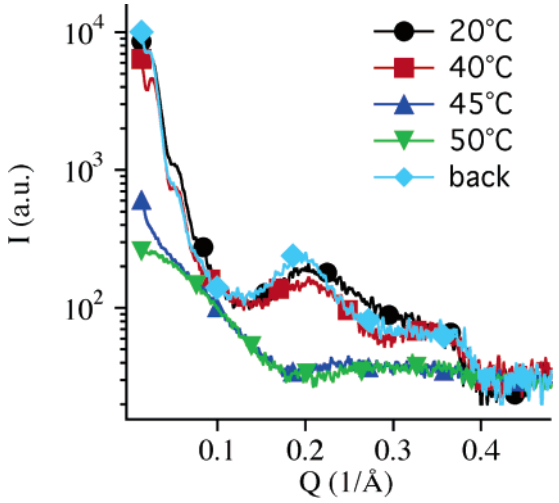

Figure 8. SAXS intensity distribution for the 10% w/w sample as a function of temperature, between 20 and 50 °C.

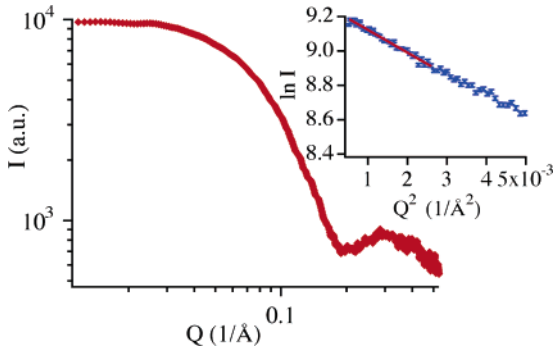

Figure 9. SAXS intensity distribution for the 5% w/w sample at 50 °C. Guinier plot ln[$I(Q)$] vs Q^2 is shown in the inset along with the resulting linear fit.

radius R_{eff} = 25.7±1.9 Å. It is important to recall that the Guinier analysis does not provide information on the shape of the scattering objects. However, in our case, the plots of ln[$I(Q)Q$] and ln[$I(Q)Q^2$] vs Q^2 excluded the existence of cylinders or disks in the Q range investigated.

Considering that the length of the polar heagroup is approximately 6 Å[26] and that the volume of a single $-(CH_2)_{10}-$ chain is about 296.4 Å^3 calculated according to the Tanford's rule,[33] the aggregation number (g) and the area per polar headgroup (a_P) can be estimated from the value of R_{eff}. In particular, g and a_P come out to be 240 and 52.6 Å^2, respectively. The interfacial free energy gain due to the formation of the micellar interface is given by $\Delta G_{surf} = 2ga_P\sigma$, where σ is the interfacial tension of a water/*n*-decane interface at 50 °C (about 50 erg/cm^2).[34] Per single monomer, $\Delta G_1 = \Delta G_{surf}/g$ turns out to be about 3.9 × 10^{-13} erg. The trans-to-gauche transition for a linear alkane requires no more than 0.97 × 10^{-13} erg/molecule. This shows that the free energy gain due to the formation of the micellar interface is about 5 times larger than the energy required to bend the aliphatic chain in the gauche conformation. This calculation and the SAXS results suggest the presence of nearly spherical micelles where the surfactant chains are closely packed in a stretched or in a bent conformation.

DSC. DSC thermograms were recorded for BOLA12/water samples to study their phase behavior between 0.05% and 40% w/w. For concentrations above 0.55%, the heat flow vs temperature curves showed an endothermic peak that corresponds to the reversible condensed-to-fluid phase transition with no hysteresis. The values of the transition temperature, T_{trans}, and of the phase transition enthalpy change, ΔH_{trans}, are shown in Table 1. T_{trans} was obtained as the temperature of the endothermic peak. ΔH_{trans} and ΔH_{exp} were determined by integrating the heat flow curves reported in Figures S2 and S3 in the Supporting Information.

The total condensed-to-fluid phase enthalpy change, ΔH_{trans}, can be divided into three contributions: the enthalpy change associated with the conformational and/or packing change of the hydrocarbon tails, ΔH_{chain}, and the changes due to the hydration (ΔH_{hydr}) and to the electrostatic interactions involving

(33) Tanford, C. *J. Phys. Chem.* **1972**, *76*, 3020−3024.
(34) Zeppieri, S.; Rodrìguez, J.; Lòpez de Ramos, A. L. *J. Chem. Eng. Data* **2001**, *46*, 1086−1088.

Table 1. Temperature ($T_{trans} \pm 0.5$ °C) and Enthalpy Change ($\Delta H_{trans} \pm 5$ J/g_{SURF}) for the Condensed-to-Fluid Phase Transition of BOLA12/Water Samples[a]

P	T_{trans}	ΔH_{trans}	ΔH_{exp}	W_b	*N*	*P*	T_{trans}	ΔH_{trans}	ΔH_{exp}	W_b	*N*
0.81	37.9	58.0				4.96	41.2	111.4			
1.26	39.0	69.8				5.53	41.6	113.6	317.3	4.9	13
1.74	39.6	84.9				10.08	42.1_5	111.2	303.9	8.9	12
2.50	40.2	107.4				18.98	42.7	109.1	287.8	13.8	9
3.02	40.6	110.2				41.32	43.7_5	102.8	233.8	29.9	7

[a] Enthalpy of melting of bulk water ($\Delta H_{Exp} \pm 0.5$ J/g_{water}), percentage of bound water over the entire water content ($W_b \pm 0.2\%$), and number of water molecules per polar headgroup ($N \pm 1$) calculated from eqs 3 and 4

the polar headgroups (ΔH_{el}):[23,35]

$$\Delta H_{trans} = \Delta H_{hydr} + \Delta H_{el} + \Delta H_{chain} \quad (2)$$

On heating, the polar headgroups release the protons (taking up ΔH_{el}). Both anionic groups and counterions then become hydrated, with the release of ΔH_{hydr}. Finally ΔH_{chain} is taken up by the hydrophobic tails to rearrange into a more fluid phase. Our results indicate that all contributions increase in absolute value with increasing surfactant concentration. Between 5% and 40% w/w, the exothermic ΔH_{hydr} contribution becomes the predominant contribution as shown by the decrease in ΔH_{trans}.

As for ASC*n*,[26] calorimetric studies on BOLA12 show the presence of two types of water in the condensed phase: a minor fraction of strongly bound water molecules, and bulk water. While the latter melts at around 0 °C, the hydration water is essentially "frozen" and remains strongly bound to the surfactant headgroups. Samples were first cooled quickly to −90 °C to avoid separation of ice from the dispersion. They were then heated to a temperature above T_{trans}. Changing the cooling/heating rates of the samples did not result in different thermal behaviors.[26] As reported previously, the percentage of strongly bound water over the whole water content, W_b (%), can be calculated from the decrease of the area of the endothermic peak associated with the melting of bulk water. The number of such strongly bound water molecules per polar headgroup, *N*, can be calculated from W_b (%) according to the following equations:[26]

$$W_b(\%) = \left(\frac{333.79 - \Delta H_{exp}}{333.79}\right)100 \quad (3)$$

$$N = W_b\left(\frac{100 - P}{2P}\right)\left(\frac{M_n}{100M_w}\right) \quad (4)$$

where 333.79 J/g is the heat of melting of pure water as reported in the literature,[36] ΔH_{exp} (in J/g_{water}) is obtained from the measured peak area normalized to the amount of water in the sample, P is the mass percentage of BOLA12 in the sample, M_w is the molecular weight of H_2O, M_n the molecular weight of BOLA12, and *N* is the number of strongly bound water molecules per polar headgroup. The values of *N* show that each headgroup in the bolaamphiphile is strongly interacting with about 10 molecules of water. Similar findings were obtained for the single-headed ASC12 surfactant.[26] This result appears to be reasonable for the chemical structure of BOLA12 and supports the predominant role played by the headgroups in the formation of the multilayered tubular nanoassemblies as shown in Figure 7. This evidence is in agreement with previous reports.[37−39]

One of the most striking features of these supramolecular nanoassemblies is the sharp monodispersity of their diameter, as shown in Figures 2 and 3. This is a typical behavior of tubules, as already reported in the literature and discussed by Selinger[40] and Boden.[41]

The formation of rodlike, helical, or planar structures is regulated by a mechanism that involves the chemical nature of the individual molecules and the interactions that they produce.[40−42] In particular, chiral molecules can aggregate and form highly packed, tilted structures. Eventually, these can assemble and form multilayered objects with high curvature. The balance between the twisting of the ribbons and the interlayer interactions limits the internal curvature of the nanotubes, and therefore controls their size and monodispersity.[41]

In our case, BOLA12 possesses some crucial structural features:

(1) it bears chiral headgroups

(2) the polar headgroups are quite bulky, with a five-membered rigid ring

(3) the headgroups carry three hydroxyl residues and four other oxygens that can readily establish intermolecular hydrogen bonds

(4) the C_5 and C_6 carbon atoms, as well as O_6 and the C═O ester group can rotate around the σ bonds and give rise to different conformations (flexibility)

(5) the hydrophobic chain contains 10 methylene groups, with some degree of lateral freedom, that can partially twist and form kinks.

These structural properties of the surfactant molecules and the interactions that they can establish (hydrogen bonding between headgroups and with water, and van der Waals interactions between the alkyl chains) contribute to the formation of the hollow, elongated, pretty monodisperse nanotubes that are shown in the cryo-TEM pictures.

Reducing Properties. The evaluation of the reducing activity according to the DPPH method indicates for BOLA12 a value of 94%, comparable to that of the native ascorbic acid and of its most common esters (between 90% and 97%).[22] This large reducing power can be exploited for the reduction of Pd^{2+} ions on the outer surface of the nanostructures. By performing the Pd coating according to the procedure explained in the Experimental Section (see Supporting Information), SEM micrographs (see Figure 10) show the presence of several nearly flat, elongated structures with a width ranging between 250 and 870 nm. The occurrence of such objects—that show a regular coating of palladium (from EDS analysis)—can be related to the formation of bundles made up of smaller assemblies. Spherical nanoparticles of palladium, with an average diameter of about 70−160 nm, are grouped in clusters.

(35) Kodama, M.; Seki, S. *Adv. Colloid Interface Sci.* **1991**, *35*, 1−30.
(36) Dean, J. A. *Lange's Handbook of Chemistry*; McGraw-Hill Book Company: New York, 1985.
(37) Shimizu, T.; Hato, M. *Biochim. Biophys. Acta* **1993**, *1147*, 50−58.
(38) Fuhrhop, J.-H.; Helfrich, W. *Chem. Rev.* **1993**, *93*, 1565−1582.
(39) Spector, M. S.; Easwaran, K. R. K.; Jyothi, G.; Selinger, J. V.; Singh, A.; Schnur, J. M. *Proc. Natl. Acad. Sci. U.S.A.* **1996**, *93*, 12943−12946.
(40) Selinger, J. V.; Spector, M. S.; Schnur, J. M. *J. Phys. Chem. B* **2001**, *105*, 7157−7169.
(41) Nyrkova, I. A.; Semenov, A. N.; Aggeli, A.; Boden, N. *Eur. Phys. J. B* **2000**, *17*, 481−497.
(42) Frankel, D. A.; O'Brien, D. F. *J. Am. Chem. Soc.* **1994**, *116*, 10057−10069.

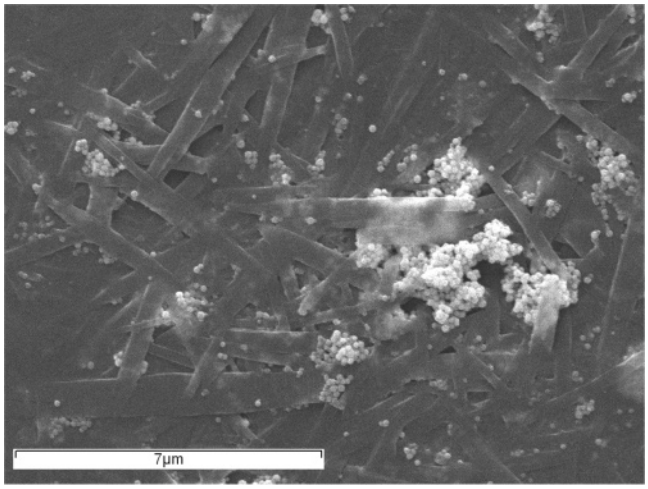

Figure 10. SEM micrograph of a BOLA12/water (2% w/w) sample treated with $PdCl_2$.

This result indicates that the external surface of the nanoassemblies can act as an efficient reducing substrate for appropriate metal cations. The exploitation of this system as template for the fabrication of metal nanowires and other assemblies could be useful for the production of molecular electronic devices and is currently under investigation.

Conclusions

1,12-Diascorbyl dodecanedioate, BOLA12, is a bolaform surfactant that bears two redox-active vitamin C headgroups. This molecule forms stable self-assembled nanotubes in water at room temperature, that turn into clear micellar solutions upon heating. The structure and size of the nanoassemblies have been assessed through cryo-TEM, XRD, and SAXS experiments. The nanotubes are made up of several layers of BOLA12 molecules and show an outer diameter of about 25 nm. The condensed-to-fluid phase transition has been studied by conductivity and DSC. These measurements indicate that the phase transition is dominated by the interactions involving vitamin C headgroups. Each hydrophilic head is hydrated on the average by 10 strongly bound water molecules, which contribute to the formation of the tightly arranged surfactant layers. Because of the presence of ascorbic acid rings in the molecular architecture, the nanotubes perform an efficient reducing activity that leads to the formation of a homogeneous thin layer of palladium on their outer surfaces. This result can be exploited for the production of nanosized metallic materials and is the subject of future investigations.

Acknowledgment. We acknowledge the Consorzio Interuniversitario per lo Sviluppo dei Sistemi a Grande Interfase (CSGI, Florence), and the Ministero dell'Istruzione, dell'Università e della Ricerca (MIUR, Rome) for partial financial support.

Supporting Information Available: Details for the synthesis of BOLA12 and general procedures for sample preparation and for experimental measurements. This material is available free of charge via the Internet at http://pubs.acs.org

JA057730X